Synthesis, Structure, and Properties of a New Analogical Molecular Perovskite Energetic Material $[(C_{14}H_{31}N_4)(ClO_4)_3]$

Xiaolan SONG[a,*], Yi WANG[b,*], Chongwei AN[a], Fengsheng LI[c]

[a] School of Environment and Safety Engineering, North University of China, Taiyuan 030051, China

[b] School of Materials Science and Engineering, North University of China, Taiyuan 030051, China

[c] School of Chemistry and Chemical Engineering, Nanjing University of Science and Technology, Nanjing 210094, China

*Corresponding author: songxiaolan00@126.com (Xiaolan SONG); wangyi528528@nuc.edu.cn (Yi WANG)

Abstract: *Molecular perovskite energetic material DAP-4, i.e. $(H_2dabco)[NH_4(ClO_4)_3]$, is a very excellent explosive, but its friction sensitivity is too high and the raw materials are slightly expensive. Therefore, in order to obtain an explosive with performance close to DAP-4, lower sensitivity and cost than DAP-4, and a structure similar to DAP-4, a novel analogical molecular perovskite energetic material, NP-1, was synthesized via a common reaction between an acid and an amine. The single-crystal diffraction results indicate that the molecular formula of NP-1 is $C_{14}H_{31}N_4O_{12}Cl_3$ or $[(C_{14}H_{31}N_4)(ClO_4)_3]$. NP-1 belongs to the orthorhombic crystal system and Pnma space group; each unit cell contains eight $C_{14}N_4H_{34}$, six guest water molecules and twenty-four perchlorate ions (ClO_4^-). The unit cell parameters are a=25.154(2) Å, b=9.5094(8) Å, c=19.7867(14) Å, and α=β=γ=90°. The results of XRD analysis and mass spectrometry analysis verified the finds from single crystal diffraction analysis. DSC analysis indicates that the thermal decomposition temperature of NP-1 is 211°C, and the activation energy for thermal decomposition of NP-1 is 241.6 kJ/mol. NP-1 has the characteristics of low sensitivity, easy availability of raw materials, simple preparation process, and low cost. Thus, NP-1 is more suitable for large-scale production during emergencies to compensate for the shortage of main explosives than the molecular perovskite energetic material DAP-4.*

Introduction

Molecular perovskite energetic materials with the ABX_3 framework have garnered significant attention over the past five years owing to their straightforward synthesis and remarkable efficacy. In 2018, Academician Chen pioneered the design and synthesis of this high-energy compound with a molecular architecture [1, 2]. For DAP-4, the A site is occupied by a protonated triethylenediamine cation (H_2dabco^{2+}, designated $C_6H_{14}N_2^{2+}$), the B site is NH_4^+, and the X site is represented by anion of ClO_4^-. This innovative ABX_3 structure combines the fuel (A site)(H_2dabco^{2+}) and oxidizer (X site) (ClO_4^-) commonly found in propellants and pyrotechnics, thereby establishing optimal conditions for their redox reactions. When NH_4^+ (B site) is oxidized by ClO_4^-, the reaction will release substantial gas and heat. Consequently, $(H_2dabco)[NH_4(ClO_4)_3]$ (i.e. DAP-4) has emerged as the most extensively investigated molecular perovskite energetic material in recent research [3-6].

However, due to the high friction sensitivity of DAP-4, the purpose of this article is to prepare a new explosive with a similar structure to DAP-4 using a closed method. The new explosive we prepared has lower sensitivity than DAP-4 and similar energy performance as DAP-4. Similar to H_2dabco^{2+}, 1,7-

Article Details ***Article No:- 0129***

Manuscript Received:- 27/05/2025 ***Final Revisions:- 10/06/2025***

Publication Date:- 11/06/2025 ***Archive Reference:- 2246***

biisopropyl-1,4,7,10-tetraazacyclododecane ($C_{14}H_{32}N_4$) can also serve as an organic fuel in molecular perovskite energetic materials and is more economical than H_2dabco^{2+}; its cost-effectiveness reduces the expenses of explosives while maintaining their efficacy.

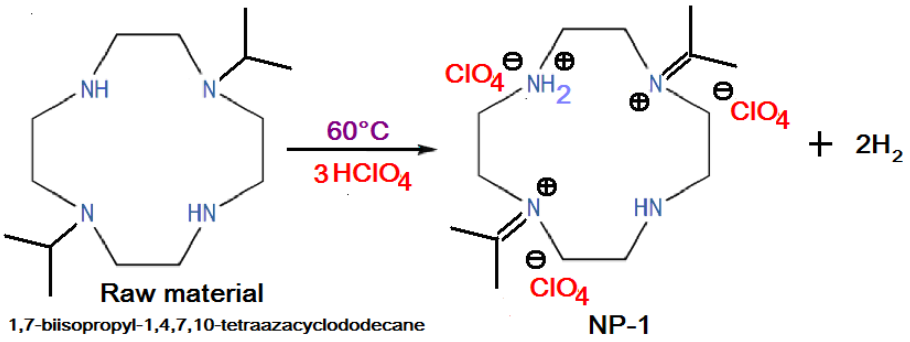

Figure 1. The synthesis path of NP-1

Both 1,7-biisopropyl-1,4,7,10-tetraazacyclododecane and perchloric acid are affordability and ready availability. Their interaction is mild and stable, producing negligible heat. The preparation process is straightforward and has a high yield, making it well suited for large-scale production. Consequently, this study selected 1,7-biisopropyl-1,4,7,10-tetraazacyclododecane ($C_{14}H_{32}N_4$) as an organic fuel, reacting it with the oxidizing agent $HClO_4$ to synthesize a novel class of elemental explosives. The structural characteristics, thermal decomposition behavior, and energetic performance of this innovative explosive were thoroughly analyzed. These findings offer a crucial foundation for ensuring the availability of high explosives in emergency scenarios during emergencies. Both 1,7-biisopropyl-1,4,7,10-tetraazacyclododecane and perchloric acid are affordable and readily available.

Materials and methods

Here, the planned product is named NP-1 in advance, and its synthesis pathway is shown in Figure 1. The reaction mechanism is easy, i.e., some 1,7-biisopropyl-1,4,7,10-tetraazacyclododecane undergoes ion displacement reaction with some perchloric acid in an aqueous solution at 60°C, which is a simple reaction between an acid and an amine compound, resulting in the formation of a precipitate and some hydrogen gas, namely NP-1 and H_2. The specific preparation process is as follows: First, 0.1mol of 1,7-biisopropyl-1,4,7,10-tetraazacyclododecane was completely dissolved in 300 mL of deionized water to form solution **A**. Second, 0.3mol perchloric acid (35 wt.%) was added to solution **A,** forming solution **B.** Third, solution **B** was heated in a water bath to 60°C and maintained for 1 hour. Fourth, the holding flask was removed from the water bath and poured into a 200 mL beaker. When the solution in the beaker cooled to approximately 0 °C, all white precipitate was filtered out and washed twice with ice distilled water. Fifth, the filtered precipitate was placed in a -45°C refrigerator and frozen for 24 hours. The frozen precipitate was then vacuum sealed and freeze-dried in at -50°C for 48 hours, finally yielding NP-1 in white powder form. During preparation, if the temperature of the refrigerator is greater than -45 °C, poor dispersion of the product NP-1 will occur after freeze-drying, resulting in especially uneven particle sizes due to agglomeration. Only when the refrigerator temperature is below or equal to -45 °C can NP-1 powder have good dispersibility with no clumping. Overall, the preparation process of NP-1 has a relatively low temperature (only 60°C), and the reaction process is simple with only one step; Moreover, the yield is high and the raw materials are affordable and readily available; the waste liquid is minimal, non-toxic, and easy to handle. The yield of NP-1 is 90%. In summary, the preparation of NP-1 is a fairly simple and inexpensive process. Therefore, NP-1 is a promising high-energy explosive candidate to substitute when Hexogen is not available.

Scanning electron microscopy (SEM) images were taken using the a TESCAN MIRA3 system, the elemental composition of the

samples was checked via energy dispersive spectroscopy (EDS), and the samples were sprayed with gold using an ion sprayer to increase the conductivity of the samples prior to use. The elemental composition of NP-1 was analyzed using a FlashSmart elemental

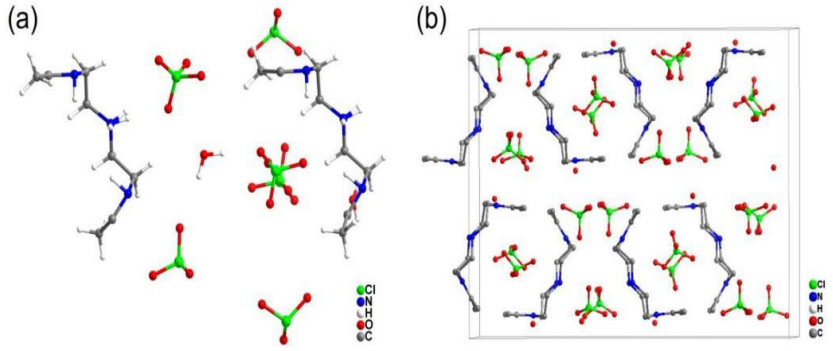

Figure 2. Molecular structure of NP-1 derived from raw single-crystal diffraction data

analyzer from Thermo Fisher. The single-crystal diffraction pattern of NP-1 was obtained via X-ray single-crystal diffraction using a Bruker D8 VEN FUTURE. Further crystal structure data of NP-1 were obtained via X-ray powder diffraction (XRD, Empyrean) with a scanning angle range of 5~90° and a scanning speed of 5°/min. The mass spectrometry was tested using a Shimadzu LCMS-IT-TOF high-resolution mass spectrometer. Thermal decomposition was studied using differential scanning calorimetry (DSC, DSC-100) with heating rates of 5, 7, 10, and 15 °C/min. The impact and friction sensitivities of NP-1 were determined via GB/T 21567-2008 and GB/T 21566-2008, respectively.

Results and discussion

To determine the molecular structure of the prepared NP-1, a single crystal was characterized using single-crystal X-ray diffraction analysis. The crystal data and structure refinement of NP-1 are presented in Table 1 and Figure 2(a and b). The molecular formula of NP-1 is $[(C_{14}H_{31}N_4)(ClO_4)_3]\cdot(H_2O)_{0.75}$, with a total element sum of $C_{14}H_{31}N_4O_{12}Cl_3$. NP-1 crystallizes in the orthorhombic *Pnma* space group with unit cell parameters: *a*=25.154(2) Å, *b*=9.5094(8) Å, and *c*=19.7867(14) Å. Each asymmetric unit contains two halves of $C_{14}H_4H_{34}$, six half-occupied perchlorates, one half-occupied and one-fourth H_2O, as illustrated in Figure 2a. Each unit cell consists of eight $C_{14}H_4H_{34}$, twenty-four perchlorates (ClO_4^-) and six H_2O (Figure 2b). Strong hydrogen bonding interactions are observed between the water molecule (O8 atom) and neighboring perchlorates, with O···O distances of 2.9332(2) Å (O7···O3), and 2.8137(2) Å (O8···O6B). The N5 atoms in the NP-1 skeleton also have hydrogen bonding interactions with the O2 atoms of perchlorate, with an N···O distance of 2.9699(2) Å. Moreover, using raw single-crystal diffraction data and specialized software, we have derived the molecular structure formula of NP-1, as shown in Figure 1. The molecular structure of NP-1 closely resembles that of its precursor, 1,7-biisopropyl-1,4,7,10-tetraazacyclododecane ($C_{14}H_{32}N_4$).

We performed SEM and EDS analyses on the prepared NP-1 sample, with results shown in Figure 3. The SEM images in Figure 3a and b reveal that the microstructure of NP-1 consists of square and strip-shaped particles with sharp edges. The EDS spectra in Figure 3c-g confirm that the prepared NP-1 is composed of a uniform distribution of four elements: C, N, O, and Cl. Since the EDS spectrum cannot detect hydrogen, there is no EDS spectrum of H in Figure 3. This finding confirms that the prepared NP-1 matches the expected molecular composition. Additionally, we performed X-ray diffraction (XRD) analysis on the prepared sample. We compared the measured XRD patterns with those simulated from single-crystal diffraction data. The results are shown in Figure 3. Figure 3 shows that the peak positions in the measured XRD pattern are consistent with those in the simulated XRD pattern. This result further confirms that the crystal structure of NP-1

measured by single-crystal diffraction analysis is consistent with the crystal structure of NP-1 measured by X-ray diffraction (XRD) analysis.

We also analyzed NP-1 using a high-resolution mass spectrometer, and the results are shown in Figure 3(j and k). As illustrated in Figure 3j,

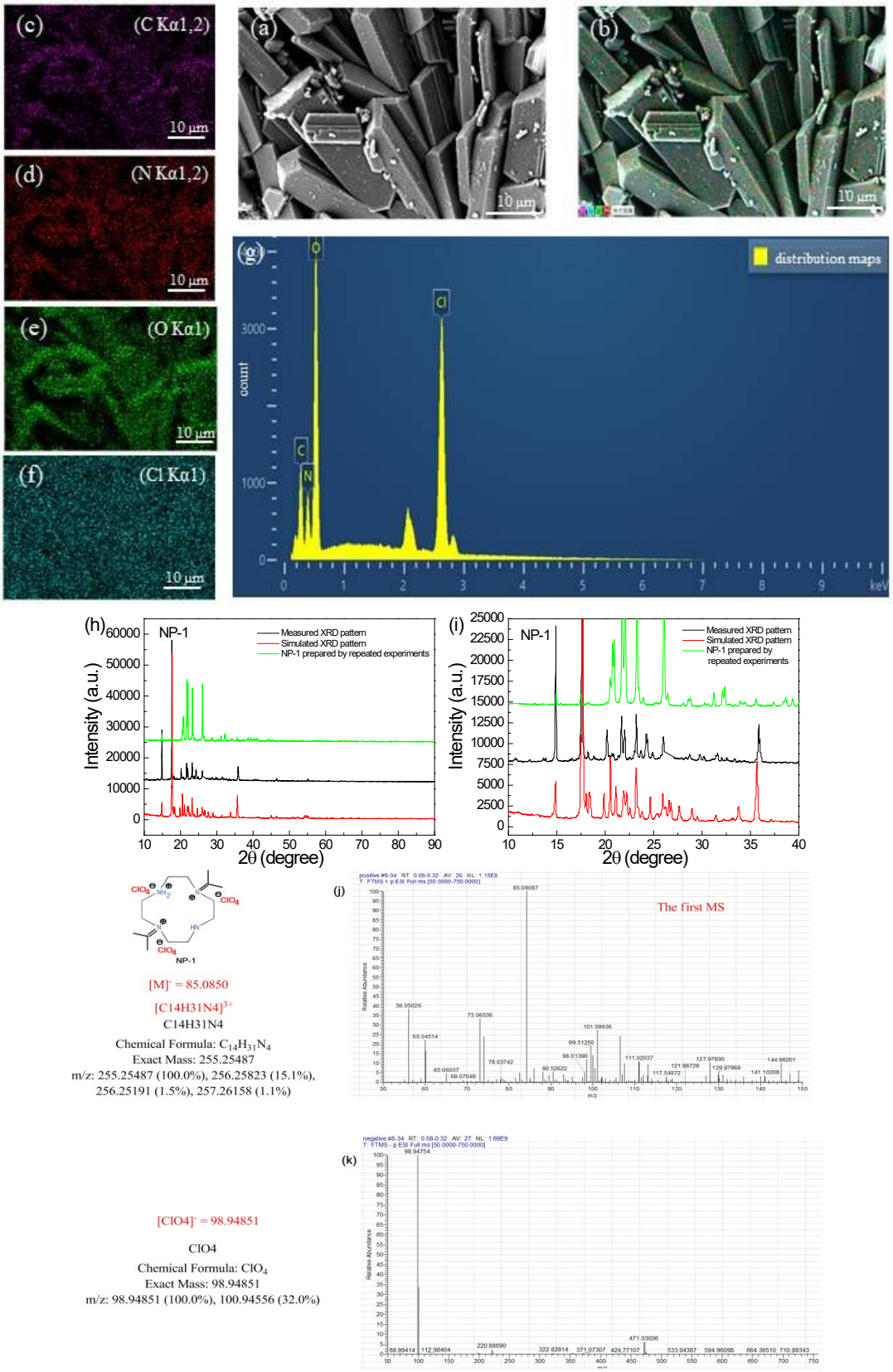

Figure 3. SEM image (a, b) and EDS spectra (c~g) of NP-1 and the experimental and simulated powder XRD patterns of NP-1 (h, i); Figure 3i is an enlarged view of Figure 3h; (j,k) mass spectrometry of NP-1

the HR-ESIMS spectrum of mimic 2 shows a strong positive molecular ion peak at m/z 255.25487 (calcd. 1084.2169 $[M]^+$), being in well accordant with its crystal structure; meanwhile, in Figure 3k, the mass spectrum of anions confirms the presence of perchlorate ions. Therefore, the result obtained from high-resolution mass

Table 1. Crystal data and structure refinement details of NP-1

Code	**NP-1**
CCDC number	2389701
formula	$C_{56}H_{130}Cl_{12}N_{16}O_{51}$
formula weight	572.83
habit	orthorhombic
space Group	Pnma
a (Å)	25.154(2)
b (Å)	9.5094(8)
c (Å)	19.7867(14) 19.7867(14)
V ($Å^3$)	4733.1(7)
Z	2
T (K)	193
λ (Å)	0.71073
2θ range for data collection/ (°)	3.838 to 52.894
Index ranges	-31 ≤ h ≤ 31 -11 ≤ k ≤ 11 -21 ≤ l ≤ 24
ρ_{calcd} (g cm^{-3})	1.592
μ (mm^{-1})	0.458
F(000)	2380.0
Crystal size/mm^3	0.12 × 0.1 × 0.09
Reflections collected	37878
Independent reflections	5173 [R_{int} = 0.0847, R_{sigma} = 0.0513]
Data/restraints/parameters	5173/175/391
GoF on F^2	1.040
R_1, wR_2 [I>=2σ(I)]	0.0815, 0.1979
wR_2 [I > 2σ(I)]	0.1685
R_1, wR_2 [all data]	0.1293, 0.2324
wR_2 (all data)	0.1968
$(\Delta\rho)_{max}$, $(\Delta\rho)_{min}$ $(\Delta\rho)_{min}$/e ($Å^{-3}$)	0.98/-0.64

Table 2. Thermodynamics, kinetics, and thermal stabilities derived from DSC traces

Samples	Thermodynamics			Kinetics		
	$\Delta H^{\neq}$ (kJ/mol)	$\Delta G^{\neq}$ (kJ/mol)	$\Delta S^{\neq}$ (J/mol·K)	E_K (kJ/mol)	lnA_K	k (s^{-1})
NP-1	237.6	120.0	242.8	241.6	60.1	1.171
DAP-4 [8]	241.7	168.6	111.0	247.2	44.6	0.593

NOTE: $\Delta H^{\neq}$ is the activation enthalpy; $\Delta G^{\neq}$ is the activation free energy; $\Delta S^{\neq}$ is the activation entropy; E_K is the activation energy for thermal decomposition calculated via the Kissinger equation [7]; A_K is the pre-exponential factor calculated via the Kissinger equation [7]; and k is the rate constant, $k=A_K \cdot Exp[-E_K/(T_p \cdot R)]$ [9, 10].

spectrometry is consistent with that obtained from single crystal diffraction.

In order to explore the thermal decomposition process and products of NP-1, DSC-IR-MS combined analysis was performed and the results are shown in Figure 4. Figure 4a shows the DSC curves of NP-1 at different heating rates. Figure 4b shows the linear fitting line of the Kissinger equation. Each DSC curve exhibits a single, large exothermic peak, corresponding to the thermal decomposition process of NP-1 at different heating rates. The peak temperature of NP-1's thermal decomposition is approximately 210°C, which

is lower than that of DAP-4 (378°C) [1]. The thermochemical parameters in Table 2 were computed using the method in Ref. [7], enabling the characterization NP-1's thermodynamic and kinetic. The results are presented in Figure 4b and summarized in Table 2. Figure 4b demonstrates a robust linear correlation between $1/T_p$ and $\ln(\beta/T_p^2)$, with a coefficient of determination (R^2)

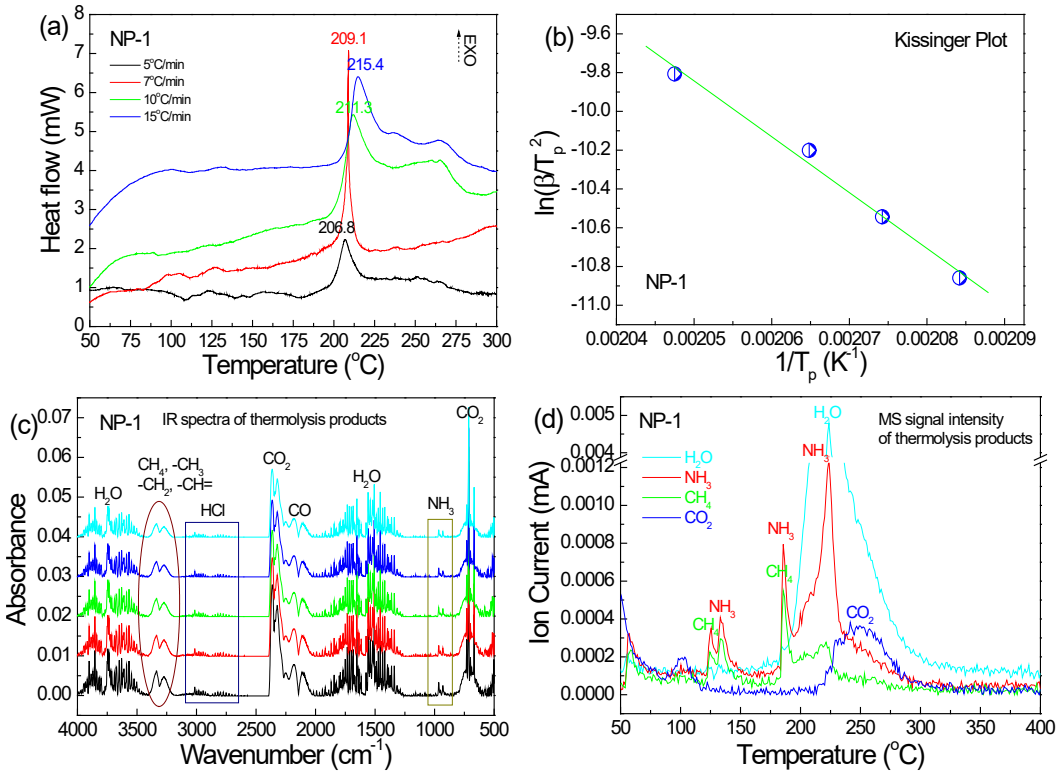

Figure 4. DSC-IR-MS combined analysis of NP-1: (a) DSC traces; (b) Kissinger plot; (c) IR spectra of gaseous products for thermal decomposition of NP-1; (d) MS signal intensity of gaseous products for thermal decomposition of NP-1

exceeding 0.99; this suggests that the activation energy and pre-exponential factor derived from the DSC data are accurate. The kinetic data in Table 2 show that the activation energy (E_K) of NP-1 is similar to that of DAP-4 [8]. However, the rate constant (k) of NP-1 is greater than that of DAP-4 [8], which implies that the thermal decomposition rate of NP-1 is faster. Thermodynamic analysis indicates that the activation enthalpy ($\Delta H^{\neq}$) values for NP-1 and DAP-4 are nearly identical, implying that their activation processes require the absorption of nearly the same amount of heat. The variations in activation free energy ($\Delta G^{\neq}$) values between the two samples are minimal, with both values being positive. This indicates that the activation processes for both NP-1 and DAP-4 are non-spontaneous and require the absorption of a specific amount of heat to reach activated state. Both recorded activation entropy ($\Delta S^{\neq}$) values as positive, suggesting an increase in the system's degree of freedom following activation and indicating the potential generation of gas during the activation process.

Figure 4c shows the IR spectrum for decomposition products of NP-1, where different colors represent spectra at different temperatures. It can be seen that there is a large amount of H_2O, a certain amount of CO_2, NH_3, HCl, and a small amount of methane in the product. Figure 4d shows the MS spectrum for decomposition products of NP-1, where different colors represent different gas products. Figure 4d indicates that the most important decomposition product of NP-1 is H_2O; In addition, it also contains some NH_3, CH_4, and CO_2, which is consistent with the results obtained from the infrared spectrum. However, in the MS test, due to the inability to select chlorine element, the generation of HCl was not reflected in the MS spectrum. But overall, DSC-IR-MS combined analysis showed that the thermal decomposition products of NP-1 are mainly H_2O, CO_2, HN_3, CH_4, and HCl,

which are consistent with their elemental composition.

The combustion heat (ΔH_c) of NP-1 was measured using a specialized calorimeter for propellants and explosives, and the enthalpy of formation (ΔH_f) was calculated using its ΔH_c value. The method for obtaining ΔH_f from the value of ΔH_c is detailedly introduced in the reference [11]. The chemical reaction equation for the complete combustion of NP-1 in excess oxygen is shown in Eq. 1. The measured ΔH_c for NP-1 is -18125.3 J/g. Using the method described in reference [11], the enthalpy of formation was calculated to be ΔH_f=-254.9 kJ/mol based on the value of ΔH_c. The comprehensive performance of NP-1 is summarized in Table 3. Table 3 shows that the ΔH_f of NP-1 is lower than that of DAP-4, resulting in slightly lower detonation velocity and heat compared to DAP-4. Moreover, the standard specific impulse of NP-1 is substantially lower than that of DAP-4. In fact, one of the most important reasons for these disadvantages is that the oxygen balance of NP-1 is much lower than that of DAP-4.

Table 3. Detonation performance of NP-1 and other explosives

Compounds	ρ (g/cm³)	ΔH_f (kJ/mol)	Q_D (kJ/kg)	VoD (m/s)	$P_{C\text{-}J}$ (GPa)	T_p (°C)	I_{sp} (N·s/kg)	IS (J)	FS (N)	OB_{CO2} (%)
NP-1	1.608	-254.9	-5933	8161	33.9	211	2417	25	105	-86.7
DAP-4 [8]	1.870	278.6	-6879	8597	35.6	378	2832	23	36	-27.9
TNT [8]	1.654	-67.0	-4022	7241	20.7	321	2059	15	353	-74.0
RDX [8]	1.820	70.7	-5844	8838	34.3	224	2617	7.5	120	-21.6
HMX [8]	1.905	75.0	-5794	9235	38.9	272	2604	7.4	112	-21.6
CL-20 [8]	2.032	415.5	-6237	9762	44.7	230	2674	5.0	84	-11.0

NOTE: NP-1 is [$(C_{14}H_{31}N_4)(ClO_4)_3$] synthesized in this work; DAP-4 is [$C_6H_{14}N_2$][$NH_4(ClO_4)_3$] synthesized in reference [1]; TNT is trinitrotoluene ($C_7H_5N_3O_6$); RDX is hexogen ($C_3H_6N_6O_6$); HMX is octogen ($C_4H_8N_8O_8$); CL-20 is hexanitrohexaazaisowurtzitane ($C_6H_6N_{12}O_{12}$); ρ is the theoretical density; ΔH_f is the tested enthalpy of formation; Q_D is the heat of detonation calculated with EXPLO5 code; ***VoD*** *is the detonation velocity calculated with EXPLO5 code; $P_{C\text{-}J}$ is the detonation pressure calculated with EXPLO5 code; T_p is the tested thermal decomposition peak temperature collected at a heating rate of 10°C/min; I_{sp} is the standard specific impulse calculated with NASA-CEA2 code; IS is the tested impact sensitivity; FS is the tested friction sensitivity; OB_{CO2} is the oxygen balance based on CO_2 for $C_aH_bN_cM_dCl_eO_f$, M as alkali metal ion, were calculated by: $OB_{CO2}[\%]=1600[f-a-(b-e+d)/2]/M_W$, where M_W is molecular weight of the explosive [1].*

$$C_{14}H_{31}N_4O_{12}Cl_3+15O_2 \rightarrow 3HCl+14CO_2+14H_2O+2N_2 \quad \text{(Eq.1)}$$

The oxygen balance of NP-1 is -86.7%, whereas the oxygen balance of DAP-4 is -27.9%. This means that for every 1 gram of NP-1 completely burned to produce CO_2, H_2O, N_2, and HCl, an additional 0.867 grams of oxygen are required, while for every 1 gram of DAP-4 completely burned to produce CO_2, H_2O, N_2, and HCl, only 0.279 grams of oxygen are needed. Thus, the result is that a significant amount of free carbon is present in the detonation and combustion products of NP-1, which does not participate in chemical reactions to release heat. The combustion and detonation of DAP-4 do not result in as much free carbon. As a result, the detonation velocity, detonation heat, and standard specific impulse of NP-1 are correspondingly lower than those of DAP-4. Figure 5 shows that, in the detonation product graph of NP-1, the mole fraction of solid carbon black is 40 mol%, which does not contribute to heat or gas moles. In contrast, the mole fraction of solid carbon black in its detonation products of DAP-4 is only 11 mol%. This comparison indirectly suggests that, compared with DAP-4, NP-1 has a consequently lower explosion heat even detonation velocity. However, energetic materials are composite materials that will contain a large amount of solid oxidizers. When more oxidizers are added to formulas containing NP-1, the explosive heat and specific impulse of formulas containing NP-1 will be similar to those containing DAP-4. Thus, for NP-1, the problem of low oxygen balance is not insurmountable. In fact, the combustion heat of DAP-4 is only -15427J/g, while the combustion heat of NP-1 reaches -18125.3 J/g, which means that the combustion heat of NP-1 is 15% higher than that of DAP-4. This indicates that, from the perspective of combustion heat, the energy performance of NP-1 is higher than that of

DAP-4. On the contrary, low oxygen balance actually brings a huge advantage to NP-1, which is low sensitivity. On the contrary, low oxygen balance gives an advantage to NP-1, low sensitivity. Our testing results disclose that NP-1 exhibits its impact sensitivity similar to TNT. The impact sensitivity is lower than DAP-4. This is a key advantage of NP-1 relative to DAP-4.

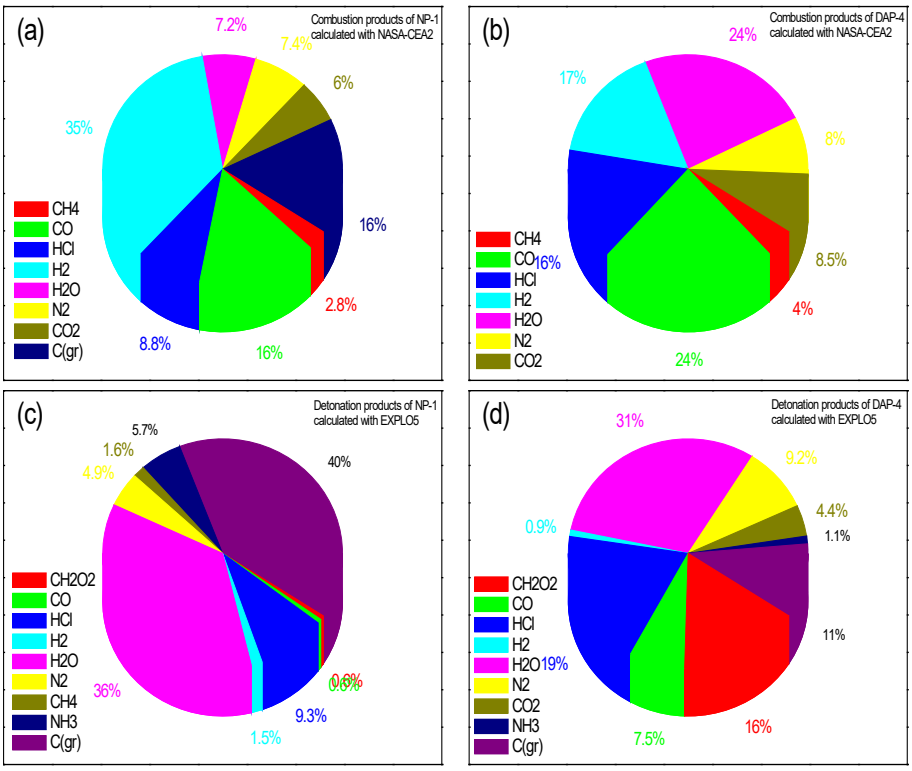

Figure 5. Molar ratios of the detonation products and combustion products of NP-1 and DAP-4

Overall, NP-1 offers low sensitivity, easy availability of raw materials, low cost, and a simple synthesis process.

Conclusions

NP-1, a analogical molecular perovskite energetic material, was synthesized using a simple method. Its chemical and crystal structures were confirmed through single-crystal diffraction, mass spectrometry analysis, and XRD analysis. The research results indicate that the thermal decomposition temperature of NP-1 is lower than that of DAP-4, but the activation energy is close to that of DAP-4. However, the rate constant of thermal decomposition of NP-1 is higher than that of DAP-4. Overall, NP-1 has the characteristics of low sensitivity, easy availability of raw materials, simple preparation process, and low cost. Thus, NP-1 is suitable for large-scale production during emergencies to compensate for the shortage of main explosives.

CRediT authorship contribution statement

Xiaolan Song: Writing – original draft, Methodology, Investigation, Data curation, Conceptualization. Yi Wang: Writing – original draft, Resources, Project administration, Investigation. Chongwei An: Software. Fengsheng Li: Writing – original draft, Conceptualization.

Declaration of competing interest

The authors declare that they have no known competing financial interests or personal relationships that could have appeared to influence the work reported in this paper.

ORCID

Xiaolan Song: https://orcid.org/0000-0001-7870-4874

Yi Wang: https://orcid.org/0000-0002-9823-6286

References

1. S. L. Chen; Z. R. Yang; B. J. Wang; Y. Shang; L. Y. Sun; C. T. He; H. L. Zhou; W. X. Zhang; X. M. Chen, Molecular perovskite high-energetic materials, *Science China Materials* Vol. 61, 2018, pp. 1123–1128
2. J. Zhou; L. Ding; F. Zhao; B. Wang; J. Zhang, Thermal studies of novel molecular perovskite energetic material $(C_6H_{14}N_2)[NH_4(ClO_4)_3]$, *Chinese Chemical Letters* Vol. 31, 2020, pp. 554–558
3. X. J. Feng; K. Zhang; Y. Shang; W. Pan, Thermal decomposition study of perchlorate-based metal-free molecular perovskite DAP-4 mixed with ammonium perchlorate, *Case Studies in Thermal Engineering* Vol. 34, 2022, p. 102013
4. E. An; Y. Tan; C. Yu; Y. Zhang; H. Liu; X. Cao; P. Deng; X. Li, Combustion performance of nano Si powder with molecular perovskite energetic materials DAP-4 as oxidant, *Vacuum* Vol. 211, 2023, p. 111916
5. P. Deng; P. Chen; H. Fang; R. Liu; X. Guo, The combustion behavior of boron particles by using molecular perovskite energetic materials as high-energy oxidants, *Combustion and Flame* Vol. 241, 2022, p. 112118
6. X. J. Feng; K. Zhang; L. X. Xue; W. Pan, Thermal decomposition mechanism of molecular perovskite energetic material $(C_6N_2H_{14})(NH_4)(ClO_4)_3$(DAP-4), *Propellants, Explosives, Pyrotechnics* Vol. 47, 2022, p. e202100362
7. Y. Wang; X. Song; D. Song; L. Liang; C. An; J. Wang, Synthesis, thermolysis, and sensitivities of HMX/NC energetic nanocomposites, *Journal of Hazardous Materials* Vol. 312, 2016, pp. 73–83
8. K. Y. Chen; X. L. Song; Y. Wang, Characterization and performance of molecular perovskite energetic material DAP-4, *Chinese Journal of Explosives & Propellants* Vol. 47, 2024, pp. 786–796
9. Y. Wang; X. Song; D. Song; C. An; J. Wang; F. Li, Mechanism investigation for remarkable decreases in sensitivities from micron to nano nitroamine, *Nanomaterials and Nanotechnology* Vol. 6, 2016, p. 184798041666367
10. Y. Kou; Y. Wang; J. Zhang; K. G. Guo; X. L. Song, Iron/aluminum nanocomposites prepared by one-step reduction method and their effects on thermal decomposition of AP and AN, *Defence Technology* Vol. 22, 2023, pp. 74–87
11. X. L. Song; Y. Wang; K. H. Jia; Z. H. Yu; D. Song; C. W. An; F. S. Li, Batch synthesis of 2,4,6-trinitro-3-bromoanisole and its thermolysis and combustion performance, *Propellants, Explosives, Pyrotechnics* Vol. 49, 2024, p. e202400009